Article no. 25

THE CIVIL ENGINEERING JOURNAL 3-2020

SEISMIC PERFORMANCE EVALUATION OF A MASONRY BUILDING SUBJECTED TO NEAR AND FAR FIELD GROUND MOTIONS

Özden Saygılı[1]

1. *Yeditepe University, Faculty of Engineering, Department of Civil Engineering, Istanbul, 34755, Turkey; ozden.saygili@yeditepe.edu.tr*

ABSTRACT

On October 23, 2011 an earthquake occurred approximately 20 km north of the province of Van, Turkey with a magnitude of Mw 7.2. Following the main earthquake, 111 aftershocks with magnitudes of 4.0 and above occurred. The state of damage was very severe and considerable amount of unreinforced masonry buildings were affected highlighting the need for investigating the seismic design of unreinforced masonry buildings in the affected area. In this paper, seismic behaviour of a two story masonry building designed according to the Turkish Building Seismic Code 2018 is presented. The main objective of this activity was to study the near field and far field synthetic ground motions, artificial ground motions and evaluating the responses to get reliable information on the seismic response of masonry buildings.

KEYWORDS

Masonry buildings, Seismic analysis, Near-field seismic motion, Time history analysis

INTRODUCTION

Located in a major earthquake zone in Turkey, most of the buildings especially in rural areas are in form of masonry construction. Historical ones are generally unreinforced stone or brick masonry. Modern masonry buildings are generally reinforced and confined masonry constructed with fired clay bricks or concrete blocks. This structural type of brick masonry is also widely used for housing in most of the countries due to its advantages of brickwork, aesthetic appearance and economy of the construction [1], [2], [3], [4]. In many countries a considerable amount of research was carried out and continues to contribute to improvement of seismic codes for masonry buildings. In Turkey, this type of construction became popular in recent times but there is no specific design code for masonry buildings. It is important to investigate the seismic behaviour of masonry buildings since large mass of walls could result in serious damages under earthquake ground motion. In this study a two-story masonry building was designed according to the recently adopted Turkish Building Seismic Code 2018 (TBSC 2018) [5]. Structural performance of the masonry building was investigated under seismic excitations. Dynamic analyses were performed under real and simulated ground motions. Near filed and far field synthetic ground motions were generated compatible with the target spectrum. Due to the characteristics of earthquakes, near field ground motions have long period velocity pulses that are not shown in far field ground motions. Besides, the effect of ground motion of a moderate-large earthquake recorded in a near-field, mostly differ from the effects recorded far from the earthquake source [6]. This research also aims to investigate the seismic response of a two-story masonry building due to near-field and far-field ground. Therefore, the City

of Van located in Turkey was chosen as the study area. The city is under the influence of the 40 km long Bitlis fault zone which passes about 20 km north of the city and the South Anatolian fault. The region of Van is under the influence of the north-south compression and contraction zone as a result of the proximity of the Arabian plate to the north towards the Eurasian plate. There are three different categories of faults falling in the Van region; strike-slip, thrust to reverse and oblique-slip normal [7]. A simplified tectonic unit and seismic activity of Van and its surroundings is given in Figure 1. These maps were constructed with Generic Mapping Tools (GMT). On October 23, 2011 the Van earthquake occurred approximately 20 km north of the province of Van with a magnitude of Mw 7.2 with a right-lateral strike-slip mechanism. Following the main earthquake, 111 aftershocks with a magnitude of Mw 4.0 and above occurred. According to the Disasters and Emergency Situations Directorate of Turkey (AFAD), this earthquake resulted in the death of approximately 604 people, 4,152 people were injured, and 6,017 buildings collapsed [8]. Another earthquake of Mw 5.7 took place on 9 November 2011. In addition to that, after October 23, 2011, 5527 earthquakes ranging in size from 1.4 to 5.7 occurred in the Van earthquake region for about 1 year [9], [10].

GROUND MOTION DATA SETS

The ground motion recorded in field within a distance of about 20 km from the fault rupture is typically known as near-field ground motion. Although there is no clear definition for the distance range of near and far field, if the site is about 50 km around the fault then the ground motion is considered as a far-field earthquake. Near-field ground motions distinctively have higher acceleration, more limited frequencies and different pulses in time histories as far as far field ground motion is concerned. In addition to that, forward directivity and fling step effects are common characteristics of near-field ground motions. These effects result from rupture mechanism, residual ground displacement and slip direction of rupture relative to the site. At the beginning of the record, large pulses are observed due to transfer of a major portion of the fault's energy to the site when the rupture propagation of the fault towards a site with a velocity close to the shear wave velocity. Seismic waves observed at site with radiation pattern of the fault oriented in the fault-normal direction get close to each other and generate a large pulse which decreases the duration of the fault waves reaching the structure [11], [12]. Although most of these pulses are observed from the radiation pattern of the fault oriented in the fault-normal direction, the fault parallel direction could result in strong pulses [13], [14]. Fling-step effect is the relative slip between the hanging wall and footwall which produces large amplitude unidirectional velocity pulse and a monotonic step in displacement time history [15], [16]. These pulses result in the occurrence of static permanent ground displacements due to tectonic deformation associated with fault rupture [17]. As these near field effects can lead to higher seismic demands, it is important to take seismic design of structures located in the near-field zone into consideration [14], [18], [19], [20], [21]. TBSC 2018 provides regional variations in the shape of the response spectrum for site conditions, earthquake source and path. In this study for the target spectrum, a reduced design acceleration spectrum was created under a horizontal earthquake effect according to the TBSC 2018. The soil profile in the selected area is composed of thick, medium solid-hard silt and silt sand and gravel sand layers ranging from clay to medium tight-tight. The shear wave velocities obtained in the central districts of Van province according to SPT-N values vary between 261.3 m / s and 357.7 m / s [22], [23]. Taking into account the site properties proposed by the National Earthquake Hazard Reduction Program (NEHRP), the site is medium tight-hard as class D [24].

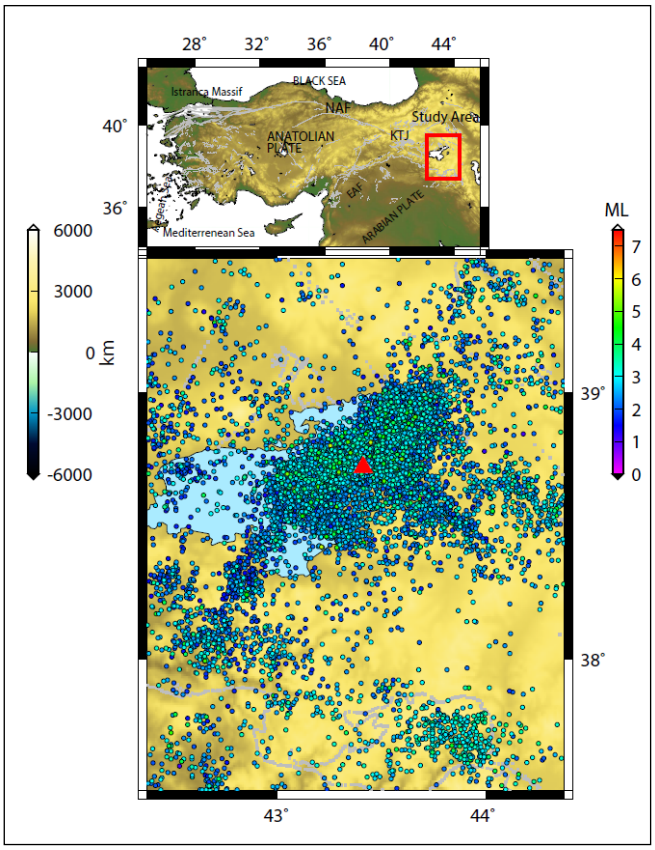

(a)

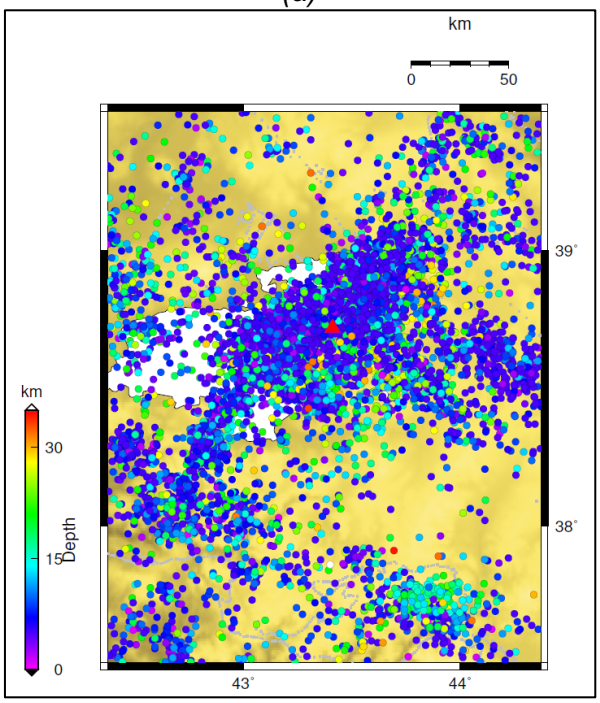

(b)

Fig. 1 – A simplified tectonic units and seismic activity of Van and surroundings

Two different earthquake ground motion levels were taken into consideration for the generation of synthetic accelerograms. The first ground motion level has a 2% probability to be exceeded in 50 years. Return period of this ground shaking is approximately 2475 years. The second ground motion level has a 10% probability to be exceeded in 50 years. Return period of this ground shaking is approximately 475 years. For each earthquake ground motion level a total of eight near field, eight far field synthetic excitations and eight artificial ground motions were generated based on the adaptation of a random process to a target spectrum of the region. SeismoArtif provides a user defined spectrum to generate artificial accelerograms [25]. The accelerogram was defined using target spectrum and adapting its frequency content using the Fourier transform. Hallodorson and Papageorgiou algorithm was used for the generation of synthetic motions applied both in the near-fault and in the far-field region [26]. The correction of the random process was performed for each iteration using Equation 1 [27]:

$$F(f)_{i+1} = F(f)_i \left[\frac{SRT(f)}{SR(f)_i}\right] \qquad (1)$$

where,
$F(f)_{i+1}$, $F(f)_i$ are the data of the accelerogram in the frequency domain;
$SR(f)_i$ is the data response spectrum relative to the accelerogram of that iteration due to frequency f.
SRT(f) is the data of target spectrum relative to the accelerogram of that iteration due to frequency f.

At each iteration a Fourier transformation was applied to move from time domain to frequency domain. In order to generate the synthetic accelerogram, Gaussian white noise was multiplied by Saragoni & Hart envelope shape [28]. Soil effects were considered as linear based on NERPH class D (Vs30 = 255 m/s). The smallest and largest periods of the target response spectrum were used to determine the frequency range within the power spectral density function. In order to establish the elastic response spectra, linear dynamic analysis was performed using Newmark integration method to solve the single degree of freedom system of equations of motion [29]. In addition to these synthetic ground motions (SGM), artificial ground motions (AGM) were generated through the use of a Saragoni and Hart (1974) envelope shape and a power spectral density function which was calculated from the velocity target spectrum of earthquake ground motion level 1 and level 2. Sinusoidal wave Equation 2 was used to generate the steady state motion:

$$W(t) = \sum_i A_i \sin(w_i t + \phi_i) \qquad (2)$$

where,
A_i is the amplitude and Φ_i is the phase angle of the i^{th} sinusoidal wave.

In order to simulate the transient behaviour for the artificial ground motions, $GM(t)$ the steady state motions were multiplied by Saragoni and Hart (1974) envelope shape, I(t) in which the phase angles are in the interval of [0 2Π], with a uniform probability distribution by Equation 3:

$$GM(t) = I(x) \sum_i A_i \sin(w_i t + \phi_i) \qquad (3)$$

For the ground motion level 1, peak ground acceleration (PGA) of near field and far field synthetic ground motions varies between 0.51 g and 0.53 g. For the same ground motion level peak ground velocity (PGV) values which are often considered as the indicator of damage potential are in the range of 0.50 m/sec and 0.76 m/sec. For the ground motion level 2, peak ground acceleration (PGA) of near field and far field synthetic ground motions is about 0.27 g. For the same ground motion level peak ground velocity values vary between 0.31 m/sec and 0.53 m/sec. Furthermore

ground motion record of October 23, 2011 Van earthquake (ML 6.7) was downloaded from the Disaster and Emergency Management Authority (AFAD) Strong Motion Database. The earthquake lasted for approximately 80 s. Acceleration time histories of Van Earthquake are given in Figure 2. Comparison of target spectrum and response spectrum of ground motions are shown in Figure 3 and Figure 4.

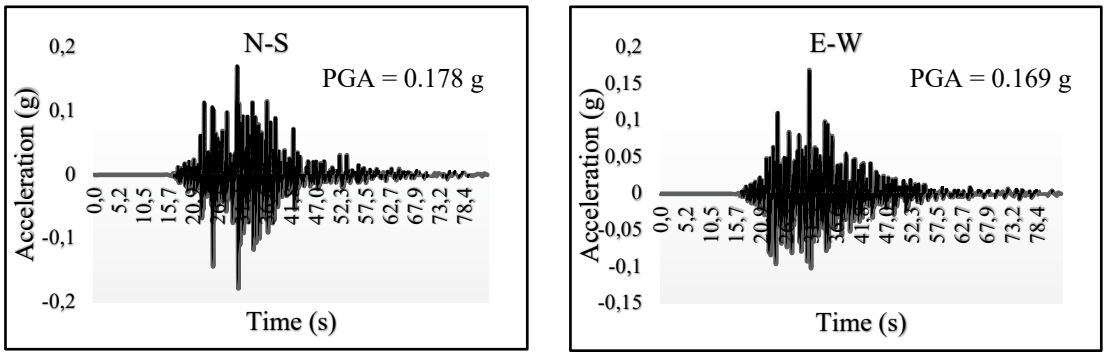

Fig. 2 – Acceleration histories of Van NS and EW components

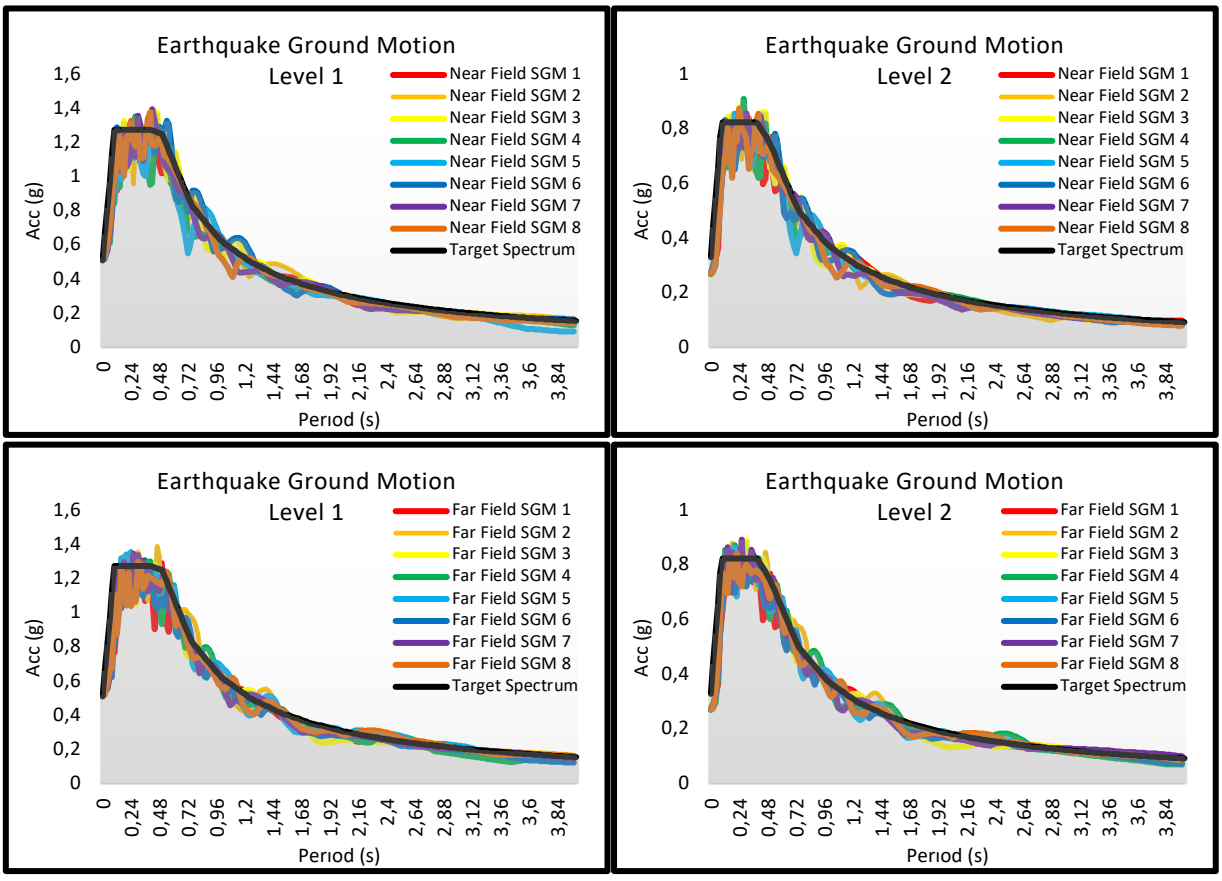

Fig. 3 – Comparison of target spectrum and response spectrum of synthetic ground motion (SGM) for ground motion level 1 and level 2

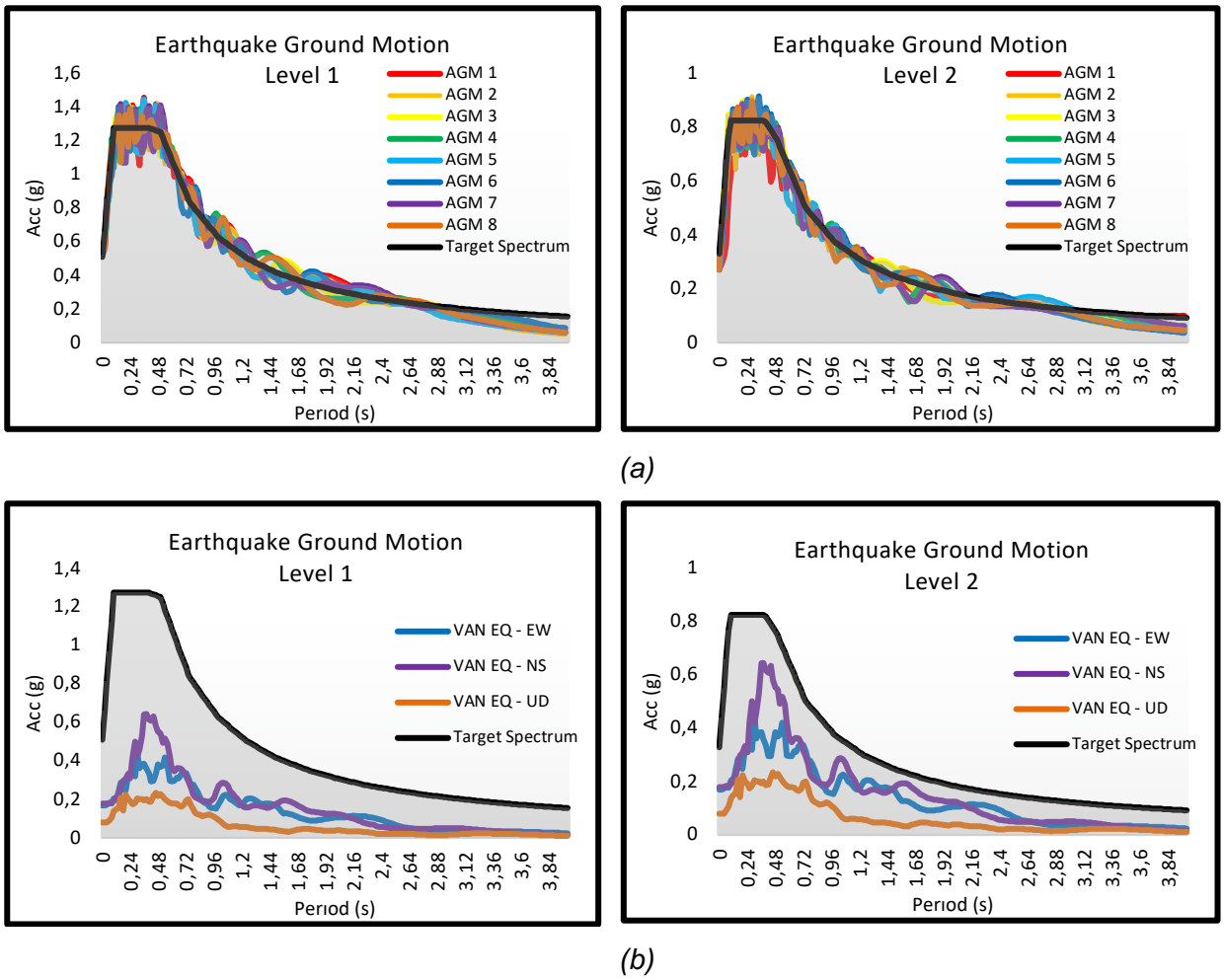

Fig. 4 – Comparison of target spectrum and response spectrum of artificial ground motion (AGM) for ground motion level 1 and level 2 (a), comparison of target spectrum and response spectrum of October 23, 2011 Van Earthquake (b)

DESCRIPTION OF NUMERICAL MODEL

For the numerical modelling, finite element modelling (FEM) software SAP2000 was used to create the two-story masonry building. The two story masonry building was considered to be designed for dead load, live load and seismic load according to the TBSC 2018. The masonry building that was considered for this study was a double story building consisting of three bays in each direction of 10.25 m long and 12 m wide. The wall was 0.25 m thick and the total height of masonry buildings was 5.90 m. In the building, tops of openings in the story were at the same level. The plan of the building consisted of a continuous lintel band through all walls just above the openings but it was not considered in the numerical model. The wall was discretized into small number of elements. The structural members of the masonry building were slabs, beams and bearing walls. The slab was reinforced concrete and was supported by horizontal beams on the masonry walls. In order to integrate concrete slab and masonry walls with each other and distribute the horizontal loads to the masonry walls; rigid diaphragm behaviour was adopted. By this way, the shear force induced by the walls was compensated by the in-plane rigidity of the walls. In the numerical model floor, the slab has a degree of freedom of translation in two in-plane directions and rotation about the vertical direction. At 4 m intervals in the masonry walls vertical beams were

designed according to TBSC 2018. These vertical beams and proper connection between wall and diaphragms would lead to ductile behaviour governed by the in plane response of the masonry walls.

In the Eurocode 8 of Part 1 and Part 3, the conditions of limit for the design or assessment of masonry buildings refer to a damage limitation and to an ultimate limit state. According to Eurocode 8, three different performance criteria are included: damage limit state of the occurrence of damage and the associated limitations of use. The Ultimate limit or Life Safety limit state that the structure should remain without global or local collapse that the structure continue to carry the gravity load demands of buildings and a residual load bearing capacity [30]. In the FEMA E-74, earthquake damage to non-structural elements are given in three types of risks: Life Safety limit state, Property Loss limit state and a Functional Loss limit state [31]. In the FEMA 273, the given performance criteria applied for structural components and unreinforced masonry infill walls are Immediate Occupancy, Life Safety and Collapse Prevention [32]. According to the given definitions for the performance of masonry buildings in TBSC 2018, if the shear strength of all the walls of the masonry building in both directions is sufficient to meet the shear forces generated by the applied earthquake effects, it is concluded that the building provides a Limited Damage Performance Level. This level of performance corresponds to the level of damage in which the building damage is limited, i.e. non-linear behaviour is limited. If the contribution of the walls that do not meet this condition to the shear force is lower than the 40% in the earthquake direction applied on any floor, the building will be considered to provide the Controlled Damage Performance Level. This level of performance corresponds to the level of damage to the structural components which is not serious and often repairable to ensure safety. If this rate exceeds 40%, the building is considered to be in a Collapse State. In this study, the resulting shear force was compared with the safety shear strength of the wall, taking into account the vertical normal force on the wall and the bearing strength of the wall. Wall areas were calculated by removing gaps such as doors and windows. For the safety of the structural system, the torsional rigidity relative to the vertical axis of the building was determined according to the TBSC 2018. Masonry walls were designed such that the stress calculated by dividing the design force acting on the masonry wall in the vertical direction by the cross-sectional area excluding door and window openings on the wall is not greater than the allowable compressive stress for the wall. In addition to that, the masonry walls were designed such that the design strength of vertical load was greater than the design normal force acting in the vertical direction to the masonry wall. To this aim, the following equations given in Table 1 were used:

Tab. 1 – Equations for the mechanical characteristics of the masonry building

<table>
<tr><td colspan="2">Characteristic shear strength of masonry wall, f_{vk}</td></tr>
<tr><td>$f_{vk} = f_{vko} + 0.4\sigma_{vertical} \leq 0.10 f_b$</td><td>Initial shear strength of masonry wall, f_{vko}
$f_{vko} = 0.30$ MPa</td></tr>
<tr><td colspan="2">Vertical compression stress</td></tr>
<tr><td>$\sigma_{vertical} = \frac{N_{Ed}}{lt}$</td><td>Axial force, N_{Ed}
Wall cross-section length, l
Wall thickness, t</td></tr>
<tr><td colspan="2">Shear strength of masonry wall design</td></tr>
<tr><td>$V_{Rd} = lt\frac{1.5f_{vdo}}{b}\sqrt{1 + \frac{N_{Ed}}{1.5ltf_{vdo}}}$</td><td>$V_{Rd} = f_{vdo}\, t\, l_c$</td></tr>
<tr><td colspan="2">$f_{vdo} = \frac{f_{vko}}{\gamma_m}$
Strength reduction coefficient, γ_m is 0.2</td></tr>
</table>

The initial shear strength of the masonry wall, fvk0 is determined according to the TBSC 2018. Accepted compressive strength of the masonry wall, fb is 20 MPa. The elasticity and shear modulus of the masonry walls was calculated according to the relationship between characteristic compressive strength of masonry wall and elasticity.

Eigen frequencies and displacement mode shapes of model are shown in Figure 5. The first period is approximately 0.067 seconds which is very close to the second mode 0.055 sec due to the almost symmetric plan those corresponds to a bending mode shape on both orthogonal horizontal planes. Mode 3 involves shear and torsional movements. Mode 1 and mode 2 are predominant translation modes that exhibit a high relative modal mass in both orthogonal direction and little or near zero in rotation. Modal analysis provided valuable information insight into the dynamic characteristics of the masonry numerical model. In addition to that, as the modal contribution to the displacement depends on the static properties of the system and the dynamic response of the system under earthquake excitation time history analyses were performed.

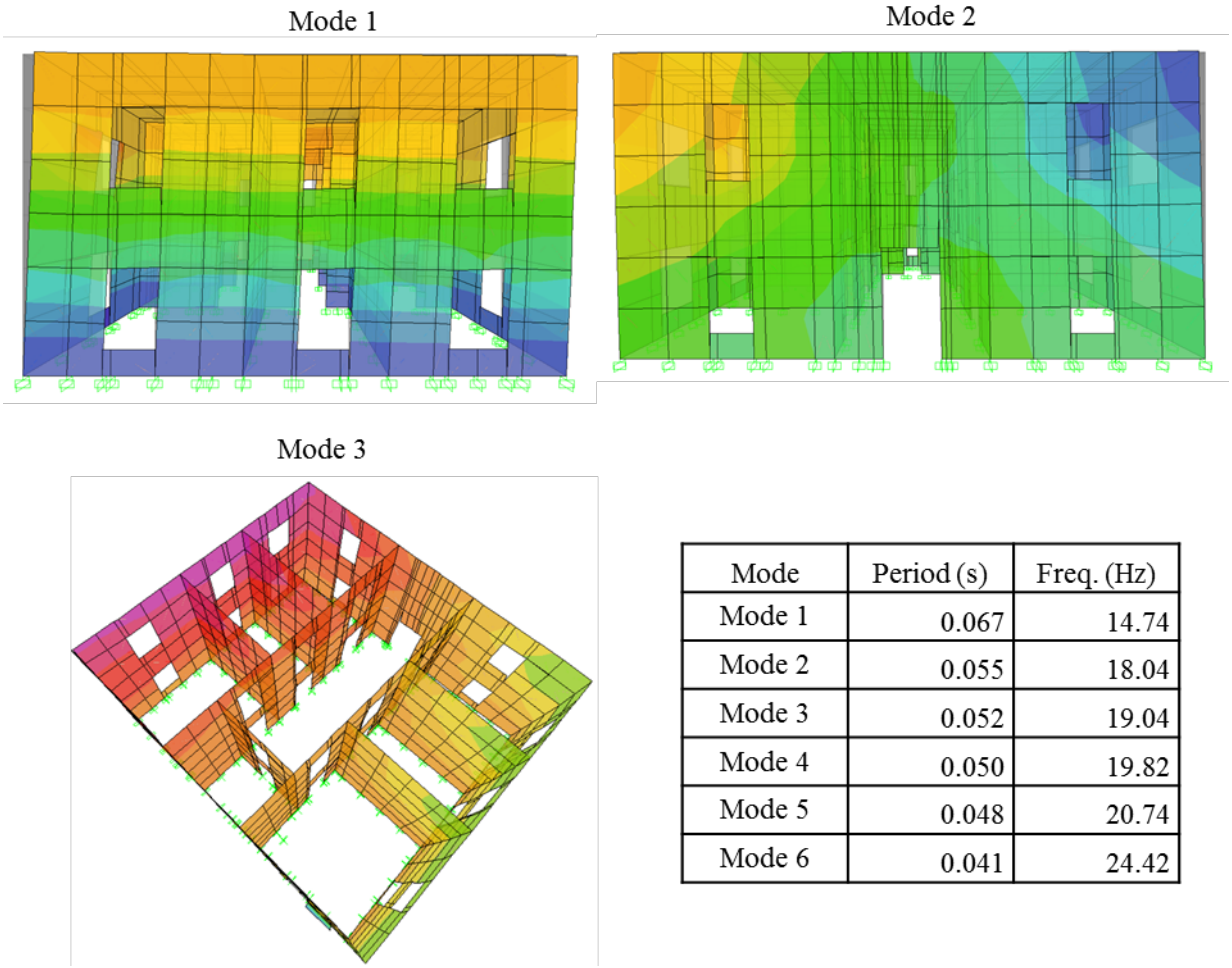

Mode	Period (s)	Freq. (Hz)
Mode 1	0.067	14.74
Mode 2	0.055	18.04
Mode 3	0.052	19.04
Mode 4	0.050	19.82
Mode 5	0.048	20.74
Mode 6	0.041	24.42

Fig. 5 – Eigen frequencies and displacement mode shapes

SEISMIC RESPONSE ANALYSIS OF A MASONRY BUILDING

Seismic ground motions were applied as base excitation to the numerical model. It was assumed that the structure was subjected to the earthquake in both horizontal directions. Due to the fact that the seismic effects in two orthogonal directions are unlikely to reach their maximum value at the same time, the 30 percent orthogonal loading rule was applied. For the time history analysis

under synthetic and artificial ground motions, 100% of the earthquake was combined with 30% of the earthquake in the orthogonal direction. During near field and far field seismic excitations, depending on the direction of ground motion, in-plane and out-of-plane forces occurred on the masonry walls. For out-of-plane, shear force and bending moment were developed in the weak direction of the masonry wall due to the weakness of the out-of-plane stiffness of the masonry wall. Horizontal inertia forces transmitted from the slab were transmitted by the in-plane forces formed on the walls in the direction of force. Under near and far field earthquakes when the torsional moment increases the shear force in one part of the masonry walls in the earthquake direction, it decreases the shear force in the other part. It created a shear force on the masonry walls for those which were not parallel to the direction of seismic loading.

Variation of top displacement and base shear force under artificial earthquakes, near and far field earthquakes for ground motion level 1 and ground motion level 2 are given in Figure 6. A brief inspection of the values indicates that the maximum roof displacements that the masonry building experienced are under near field excitations created for ground motion level 1. The duration of the artificial ground motions was about 20 sec. while for the near field and far field ground motions duration was about 10 sec. and 14 sec., respectively. As the near field ground motions have higher accelerations and more limited frequencies in time histories than the far field ground motion, the selected building experienced the highest responses in terms of deformation and stresses under near field synthetic excitations. The Masonry building was exposed to artificial ground motions for 20 sec. which resulted in the highest base shear forces in both ground motion levels. Furthermore, PGV of synthetic and artificial ground motions and roof drift ratios were compared for each ground motion set (Figure 7). Drift ratios were found by dividing the roof displacement with the story height. Considering the set of ground motion level 1; PGV of the synthetic loadings were in the range of 50 cm/sec and 76 cm/sec and PGV of the artificial loadings were in the range of 50 cm/sec and 58 cm/sec. For the second ground motion level, PGV of the synthetic loadings varied between 31 cm/sec and 53 cm/sec while PGV of the artificial loadings were in the range of 27 cm/sec and 36 cm/sec. It is evident for the near field synthetic and artificial excitations of both ground motion levels; the drift ratio increases with the increase of PGV which is not clear for far field ground motion data set. Considering the ground motion level 1, although the PGVs are in about the same range for artificial and far field ground motions, higher drifts were observed under far field loadings. Furthermore, during seismic analysis in addition to the horizontal shear forces induced in the walls in the related direction of seismic loading, under vertical loads, shear forces and bending moment occurred in slabs but shear forces were more effective on the behaviour of walls of masonry buildings than the bending moment. The designed building had damage of the ductile type distributed at many locations due to the absorption of a good amount of energy received from the seismic excitations. Close the opening tensile stresses occurred under compression which would result in cracks. As expected, the masonry structure experienced maximum tensile stresses observed under near field earthquake for ground motion level 1 and minimum tensile stress occurred under the October 23, 2011 Van Earthquake.

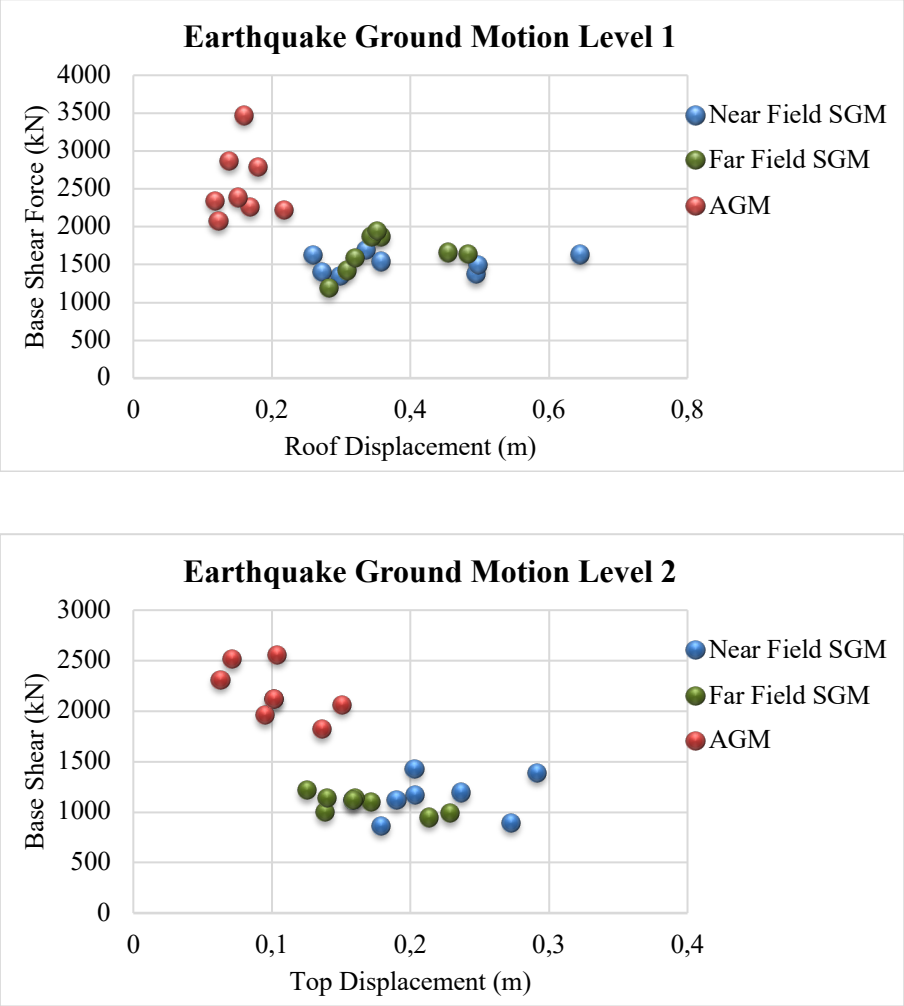

Fig. 6 – Variation of top displacement and base shear force under artificial earthquakes (AGM), near and far field synthetic earthquakes (SGM) for ground motion level 1 and ground motion level 2

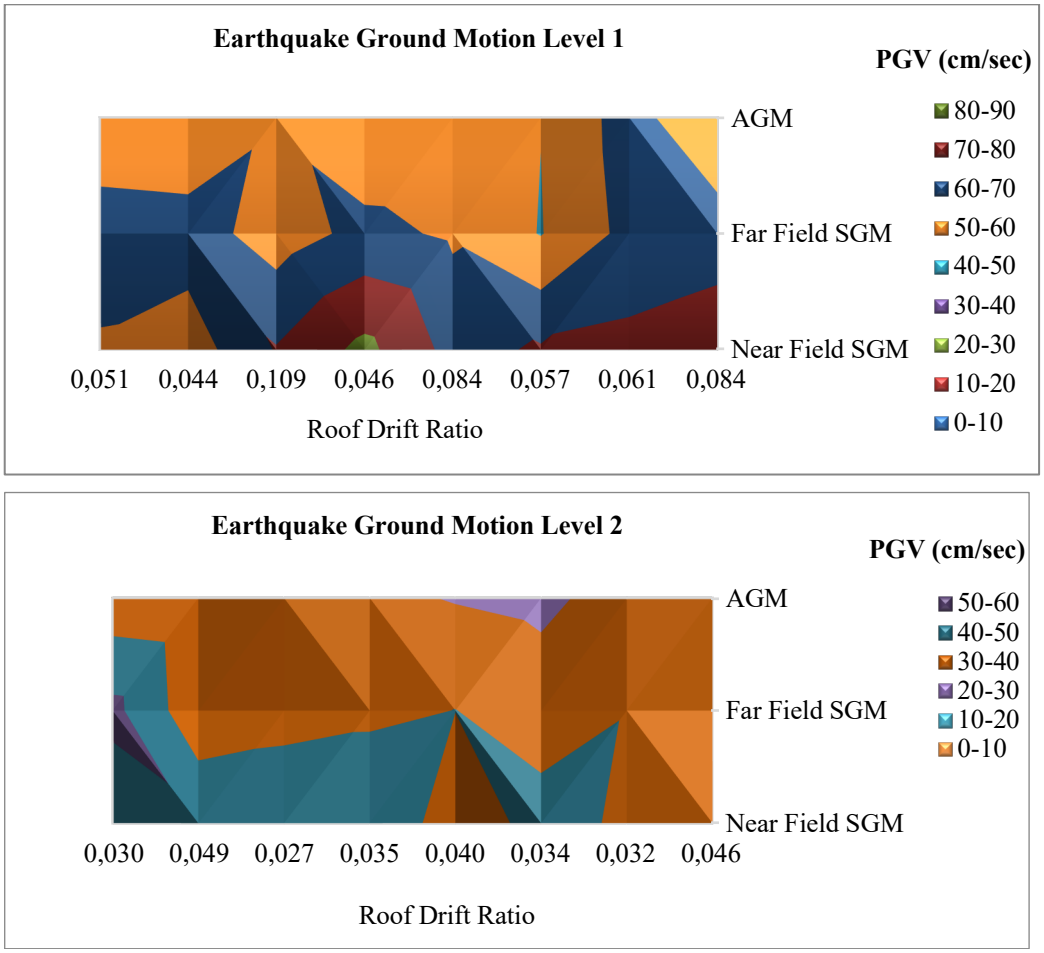

Fig. 7 – Variation of drift ratio and peak ground velocity (PGV) under artificial earthquakes (AGM), near and far field synthetic earthquakes (SGM) for ground motion level 1 and ground motion level 2

CONCLUSION

The response of masonry buildings subjected to seismic excitations depends basically on their failure mechanism and deformation characteristics. Considering the in-plane response of sliding shear failure of the masonry wall, displacement capacity was generally very large. When the principal tensile stress exceeds the in-plane tensile strength of the masonry wall, diagonal shear mode occurs. This case can be described by loss in strength and stiffness of masonry wall with limited displacement capacity. Another failure mechanism of flexural failure occurs generally in slender masonry walls due to the large ratio of moment to shear. In addition to these failure modes, rocking response can be observed due to second order effects. This study evaluates the seismic capacity of two story masonry buildings designed according to the TBSC 2018. In addition to the capacity curves determined by pushover analyses performed in two principal directions, time history analyses were also performed which led to the following conclusions:

- Near field ground motions is characterized by long period velocity pulses due to the directivity effect and the permanent tectonic deformation at the site which is referred to as the fling effect. Therefore, slender structures such as masonry minarets or towers with long natural time periods could be subjected to larger seismic demands under near field seismic excitations. But the inspection

of the results indicates that these effects could also be accounted for the selected non slender masonry building with a short natural time period.

- The maximum roof displacements that the masonry building experienced under near field excitations created for ground motion level 1 were significantly higher than those for the other earthquakes.

- Under the lateral shear force applied at roof level, the total displacement at the same level can be considered to be comprised of a displacement of the gross wall acting as a cantilever additional deflections resulting from flexibility of piers. For the ground motion level 2, under far field excitations, artificial ground motions and the October 23, 2011 Van Earthquake, the masonry building showed closed to an elastic behaviour. On the other hand, for the ground motion level 1, under near field excitations, the masonry building showed an inelastic behaviour.

- For the two levels of synthetic and artificial near field motions considered in this study, tensile stresses observed close the openings were significantly higher than the far field responses which would result in cracks. Therefore, in the design process, the location and size of the openings should be defined to optimize the performance under ground motion. Although, for ground motion level 2 under far field excitations, artificial ground motions and the October 23, 2011 Van Earthquake masonry walls passed the range of linear elastic limit a bit, under other earthquakes the deformation levels are well beyond the elastic limit.

- It can be concluded that the selected two story masonry building designed according to the TBSC 2018 can stably withstand inelastic actions without collapse. Results indicate that near field motions play an important role in seismic resistant design of masonry structures. Near field synthetic motions produced greater displacement responses in the masonry building than far field seismic excitations. However, it should be noted that in the case of stiff soils, the reverse can happen in that far field motions can result in higher responses than near field ground motions. Therefore, more analysis results of various masonry buildings subjected to near and far field seismic motion in stiff soil are needed. Major findings should be stated with respect to relevant literature. Recommendations for future research should also be made.

REFERENCES

[1] Tomazevic M., 1999. Earthquake-resistant design of masonry buildings. Imperial College Press, London (UK).

[2] EERI/IAEE, 2000. World housing encyclopedia. Earthquake Engineering Research Institute and the International Association for Earthquake Engineering. www.worldhousing.net.

[3] El-Gawady M., Lestuzzi P., Badoux M., 2004. A Review of Conventional Seismic Retrofitting Techniques for URM. In: Proceedings, 13th International Brick and Block Masonry Conference.

[4] D'Ayala D., Bostenaru M., Goretti A., Yakut A., Tomazevic M., 2005. Application of the World Housing. Encyclopedia Geophy Res Abstr, 7, 01649.

[5] TBSC, 2018. Turkish Building Seismic Code, Prime Ministry, Disaster and Emergency Management Presidency (AFAD), Ankara.

[6] Grimaz S. and MaliSan P., 2014. Near Field Domain Effects and Their Consideration in the International and Italian Seismic Codes. Bollettino di Geofisica Teorica ed Applicata 55(4): 717-738.

[7] Koçyiğit A., 2013. New Field and Seismic Data about the Intraplate Strike-Slip Deformation in Van Region, East Anatolian Plateau E. Turkey. J. Asian Earth Science, 60,586-605.

[8] AFAD, 2011. Disasters and Emergency Situations Directorate of Turkey, 28 November 2011.

[9] KOERI, 2011. Van earthquake (Mw 7.2) evaluation report as of 27 October 2011, Bogazçi University, Kandilli Observatory and Earthquake Research Institute, 3.

[10] KOERI, 2012. Son Depremler, Kandili Rasathanesi ve Deprem araştırma Enstitüsü, Boğaziçi Üniversitesi, http://www.koeri.boun.edu.tr/ sismo/zeqmap/gmapt.asp (Son Erişim: 26 Nisan 2012).

[11] Somerville P., Smith N., Graves R., Abrahamson N. 1997. Modification of Empirical Strong Ground Motion Attenuation Relations to Include the Amplitude and Duration Effects of Rupture Directivity. Seismological Society Letters, 1(68): 180-203.

[12] Tehranizade M. and Movahed H. 2011. The Investigation of Steel Moment-Resisting Frames in Tall Structures in Near-Fault Range. Journal of Civil Engineering and Mapping, 5(44): 621-633.

[13] Bray JD., Rodrigues-Marek, A., 2004. Characterization of Forward-Directivity Ground Motions in the Near-Fault Region. Soil Dynamics and Earthquake Engineering, 11(24): 815-828.

[14] Davoodi M., Sadjadi M., 2015. Assessment of Near-Field And Far-Field Strong Ground Motion Effects on Soil Structure SDOF System. International Journal of Civil Engineering, 13.

[15] Abrahamson N. and Somerville P., 1996. Effects of the Hanging Wall and Footwall on Ground Motions Recorded During the Northridge Earthquake. Bulletin of the Seismological Society of America, 86(1B), S93–S99.

[16] Somerville P. G., 2002. Characterizing near fault ground motion for the design and evaluation of bridges. Paper presented at the Third National Conference and Workshop on Bridges and Highways, Portland, Oregon.

[17] Bozorgnia B., Bertero V., 2004.Earthquake Engineering: from Engineering Seismology to Performance-Based Engineering, Florida, CRCPress.

[18] Malhorta P., 1999. Response of Buildings to Near–Field Pulse Like Ground Motion. Earthq. Eng. Struct. Dynamics, 28(11): 1309–1326.

[19] Alavi B., Krawinkler, H., 2001. Effects of Near-Fault Ground Motions on Frame Structures. John A. Blume. Earthquake Engineering Center Stanford, California, No. 138.

[20] Rodriguez-Marek A., Bray JD., 2006. Seismic Site Response for Near-Fault Forward-Directivity Ground Motion. Journal of Geotechnical and Geoenvironmental Engineering ASCE, 1611-1620.

[21] Li S., Xie L., 2007. Progress and Trend on Near-Field Problems in Civil Engineering. Acta Seismological Sinica, 1(20): 105-114.

[22] Acarlar M., Bilgin E., Elibol E., Erkal T., Gedik İ., 1991. Van Gölü Doğu ve Kuzeyinin Jeolojisi. MTA Genel Müdürlüğü, No: 1061.

[23] Selçuk L., Aydin H., 2012. Kuvaterner Yaşlı Alüvyal Zeminlerin Kuvvetli Yer Hareketine Etkisi: 2011 Van Depremleri. Jeoloji Mühendisliği Dergisi, 36(2).

[24] BSSC, 2009. The 2003 NEHRP Recommended Provisions for the Development of Seismic Regulations for New Buildings and Other Structures, Building Seismic Safety Council, FEMA, Washington D. C.

[25] SeismoSoft 2012. SeismoArtif, version 1.0.0 2012: SeismoArtif's help system 2002–2012. Seismosoft Ltd.

[26] Halldorsson B. and Papageorgiou A. S., 2005. Calibration of the Specific Barrier Model to Earthquake of Different Tectonic Regions. Bulletin of the Seismological Society of America, 95, 1276—1300.

[27] Mucciarelli M., Spinelli A., Pacor F., 2004. Un Programma per la Generazione di Accelerogrammi Sintetici “Fisici” Adeguati Alla Nuova Normative. Proceedings of XI Congresso Nazionale L’Ingegneria Sismica in Italia, Genova, Italy.

[28] Saragoni G.R., Hart G.C., 1974. Simulation of Artificial Earthquakes. Earthquake Engineering-and Structural Dynamics, 2, 219-267.

[29] Newmark, N.M., 1959. A Method of Computation for Structural Dynamics. Journal of the Engineering Mechanics Division ASCE, 85(3): 67-94.

[30] CEN., 2004. European Standard Eurocode 8: Design of Structures for Eathquake Resistance. EN 1998-1:2004, Comitè Européen de Normalisation, Bruxelles.

[31] FEMA E74, 2012. Reducing the Risks of Nonstructural Earthquake Damages, Federal Emergency Management Agency, Practical Guide.

[32] FEMA 273, 1997. NEHRP Guidelines for the Seismic Rehabilitation of Buildings, Federal Emergency Management Agency, U.S. Department of Homeland Security, Washington DC, USA.